Understanding the Contribution of Adaptive Beamforming Combined with Ultrasound Localisation Microscopy for Super-Resolved Microvessel Mapping

Citation for published version:
Voulgaridou, V, Nicolas, B, Mcdougall, S, Arthur, L, Papageorgiou, G, Butler, M, Kanoulas, E, Diamantis, K, Lu, W & Sboros, V 2024, Understanding the Contribution of Adaptive Beamforming Combined with Ultrasound Localisation Microscopy for Super-Resolved Microvessel Mapping. in *2024 IEEE International Symposium on Biomedical Imaging (ISBI).*, 10635280, IEEE, 2024 IEEE International Symposium on Biomedical Imaging, Athens, Greece, 27/05/24. https://doi.org/10.1109/ISBI56570.2024.10635280

Digital Object Identifier (DOI):
10.1109/ISBI56570.2024.10635280

Document Version:
Peer reviewed version

Published In:
2024 IEEE International Symposium on Biomedical Imaging (ISBI)

UNDERSTANDING THE CONTRIBUTION OF ADAPTIVE BEAMFORMING COMBINED WITH ULTRASOUND LOCALISATION MICROSCOPY FOR SUPER-RESOLVED MICROVESSEL MAPPING

Vasiliki Voulgaridou[1], Barbara Nicolas[2], Steven McDougall[3], Lachlan Arthur[4], Georgios Papageorgiou[4], Mairead Butler[4], Evangelos Kanoulas[5], Konstantinos Diamantis[6], Weiping Lu[4] and Vassilis Sboros[4]

[1]Centre for Inflammation Research, Queen's Medical Research Institute, University of Edinburgh, UK.
[2]INSA-Lyon, Université Claude Bernard Lyon and CNRS, Inserm, CREATIS LYON, France
[3]Institute of GeoEnergy Engineering, Heriot Watt University, Edinburgh, UK
[4]Institute of Biological Chemistry, Biophysics and Bioengineering, School of Engineering and Physical Sciences, Heriot Watt University, Edinburgh, UK
[5]Janssen Pharmaceuticals R & D, High Wycombe, United Kingdom
[6]Institute for Digital Communications, University of Edinburgh, Edinburgh, UK

ABSTRACT

Super-resolution ultrasound imaging (SRUI) has been established to overcome the ultrasound imaging diffraction limit in mapping the vascular bed. The beamforming currently used is suitable for B-mode imaging and little is known of its suitability to generate images that are subsequently processed using SRUI algorithms. This theoretical study will use a two-parallel vessel phantom to investigate the performance of minimum variance beamformers (MV BF), that are known to provide improved lateral resolution, as combined with Ultrasound Localisation Microscopy (ULM). This is compared to conventional delay and sum (DAS) beamformers. The aim is to assess vessel recovery performance using the different beamformers and investigate the link with MB localisation performance. microvessel position definition and corresponding vessel separation estimation compared to conventional DAS BFs. The MV BF was shown to provide improvement in localisation uncertainty and vessel recovery specifically for vessel separations between 1-4 λ compared to the DAS, which showed artefact vessels at this distance range. In conclusion, the MV BF is proposed as a more suitable adjunct to ULM compared to the DAS.

Index Terms— ultrasound beamforming, ultrasound contrast imaging, super-resolution ultrasound, ultrasound localisation microscopy, minimum variance

1. INTRODUCTION

A significant amount of SRUI research concentrates on image analysis, such as ULM and microbubble tracking, while there is little research on signal processing that could boost SRUI image quality and performance. SRUI is based in localising and tracking individual microbubble contrast agents (MBs) as it is well established that their scattering can be detected individually [1]. These deploy contrast enhanced ultrasound (CEUS) modes, which typically utilise conventional BFs that are used for B-mode imaging, namely the Delay and Sum (DAS) BF [2, 3]. Adaptive beamforming (BF) research aims to improve lateral resolution [4,5], but the implication of using BF, such as the minimum variance (MV), is not understood in terms of benefit to SRUI processing outputs over the DAS BF. The aim of the current paper is to theoretically investigate this. This builds on previous fundamental work that shows that the MV BF provides a 24-fold smaller Full Width at Half Maximum (FWHM) (0.08λ) in the PSF of a single scatterer compared to the DAS, while the lateral resolution improvement, based on the separability of two scatterers was marginally below one λ for the MV and at 2.1 for the DAS [6, 7]. This suggests that there may not be a clear resolution gain (i.e., separation of two adjacent scatterers) using the MV BF instead of the DAS BF. In addition, experimental work has shown that the minimum distance for detecting two scatterers using the MV was 1.2 λ, while at the DAS could not differentiate them [6]. Thus, it is important to understand whether the marginal resolution advantage of the MV BF over the DAS leads to an improve capacity to resolve vessels at smaller distances, and whether this is an important determinant for improving SRUI image quality. A simplified in silico blood flow phantom consisting of two adjacent parallel vessels is used to investigate this problem. A key parameter of interest is the distance between the two vessels, and this is assessed in terms of vessel recovery definition and location precision. Two established BFs are compared, namely the conventional

Fig. 1. Schematic representation of the in-silico phantom of two straight vessels (red) for four different lateral separations: 100μm, 200μm, 400μm, and 1000μm. The white dots represent simulated MBs flowing through the vessels.

DAS and the MV BF as a well published representative of adaptive BFs in the literature.

2. METHODS

Four different BF methods were evaluated *in silico*, the DAS boxcar, the DAS Hanning, the temporal MV BF and the MV subband BF [6, 7] in terms of resolution improvement for super-resolution imaging and vessel recovery.

2.1. Phantom Design

The numPTI software [8] was used to design the phantom, which included two 50μm diameter parallel vessels with opposing flow and placed at different lateral separations (Fig. 1). The vessels separations ranged from 70μm to 1500μm. The MBs are represented initially as dimensionless 'particles' flowing at a set flow rate. The particle positions are used as Ground Truth (GT) information against which the performance of the detection algorithm could be evaluated in terms of localisation uncertainty (LU). An initial test on a single vessel was used to benchmark BF performance as an adjunct to ULM analysis.

2.2. US image generation

One hundred consecutive time frames were used and the US data were simulated using Field II [9, 10] and a synthetic aperture (SA) was used for transmission with frequency 8MHz (λ= 192.5μm), transmission pulse length at 2 cycles and speed of sound at 1540m/s. The phantom depth of interest was between 52-80mm. The received echo data were processed with the four BF methods: DAS boxcar, DAS Hanning, MV Temporal and MV Subband developed by Diamantis et al. [6].

As there is no satisfactory MB theoretical model that simulates well the MB non-linear behaviour, knowledge from existing image data showed that the most effective option would be to assign a range of intensities to the MB population. Although this is not realistic it does enable the image analysis below with a similar performance to the literature. This also helps address the objective of the paper by removing MB appearance related uncertainty.

2.3. Image analysis and evaluation

Ultrasound localization microscopy (ULM) methodology was used for MB detection, segmentation and localization [34]. Briefly, this uses the marker-controlled watershed segmentation [12] for distinguishing the MBs from the background. Subsequently, the localization process estimates the position of the MB using the intensity weighted Centre of Mass method. The GT location of each MB was used for the evaluation of the MB detection and localization process. The metrics used were: a. True detection (TD) rate i.e percentage of all detections that correspond to GT MBs, b. Spurious events rate i.e. percentage of detections that do not correspond to GT MBs, c. Missed events rate i.e. percentage of undetected MBs and d. Localization Uncertainty (LU) which is the root mean squared error of the distance of each localization from the GT MB location.

Finally, the detected MBs were used to generate MB number maps, i.e each pixel value is the number of detected MBs. Vessel profile histograms were then generated and used to calculate the vessel location and vessel separation which was compared with the actual separation determined by the phantom design.

.

3. RESULTS AND DISCUSSION

The experiment for a single vessel provides a TD at 100% and spurious events at 0% for all BFs. The introduction of the second vessel at 1mm distance compromised this behaviour. In general all beamformers provided TD above 80% and spurious events below 2%. The LU of the BF methods for vessel separations ranging from 70μm to 1500μm is evaluated in Fig. 2. The MV BFs provide an average LU around 50μm, while the DAS BFs demonstrate localization performance comparable to the MV for vessel separations of 1000μm and above, a lateral distance that provides well separated MBs for all BFs. The convergence of all BFs in the smallest vessel separations below 100μm, is an artefact for the case of DAS BFs as the MB echoes are in complete overlap and match that of single MBs [6],

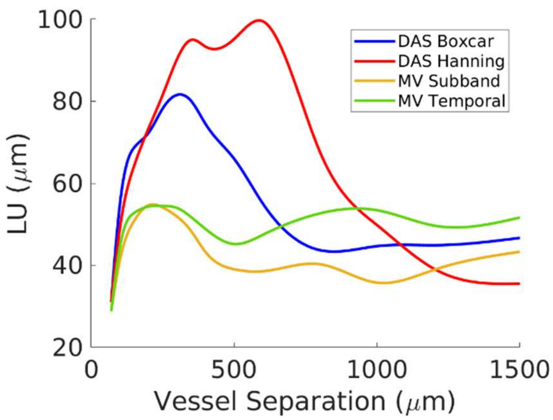

Fig. 2. LU versus vessel separation for the different BFs in the absence of noise. Vessel separation ranges between 70μm -1500μm

accompanied by an increase of missed MB events in the case of the DAS BFs. Specifically, the average missed events for the DAS for a separation of 70μm is 32% while for a separation of 1500μm is 1.7%. Note, that LU is calculated on TD data only. Therefore, the convergence of all methods at the lowest distance resembles the behaviour of the beamformers in a single vessel. Fig. 2 shows that the use of MV methods provides a clear benefit over DAS for the MB localization are between 200μm and 800μm. As explained in the introduction the DAS PSF are much larger compared to the MV and at these separations their sidelobe interaction becomes significant in compromising LU, thus resulting in increased uncertainties in LU for the DAS BFs compared to the MV beamformers. Above the nominal vessel distance of 800μm there is no longer overlap for any beamformer, and the MB PSFs are distinguished well in the segmentation processes. At these larger vessel distances the LU is similar for all BFs and it converges to their similar performance of a single vessel.

For a vessel pair at a distance of 100μm (0.52λ) Fig. 3 shows the vessel profile histograms that result from the MB number maps of the parallel vessels. It is shown that for this separation the vessels are identified as separate structures for all BFs and super resolution is achieved. In all BFs the two highest peaks correspond well to the position of the original vessels. The difference in the height of the peaks correspond to the respective number of localisations. For the DAS BF (Fig3a) there is a significant number of spurious detections that produce an artefact, erroneously identified as a vessel between the two vessels. On the other hand the MV Temporal (MVT) provides easily discernible and artefact-free vessels (Fig3b). The effect of the additional vessel is also observed for the DAS BFs for a vessel separation of 70μm, while larger separations did not produce the middle vessel artefact for any of the BFs. Overall, the MV Subband appears to provide the best agreement with the GT, up to 400μm vessel separations.

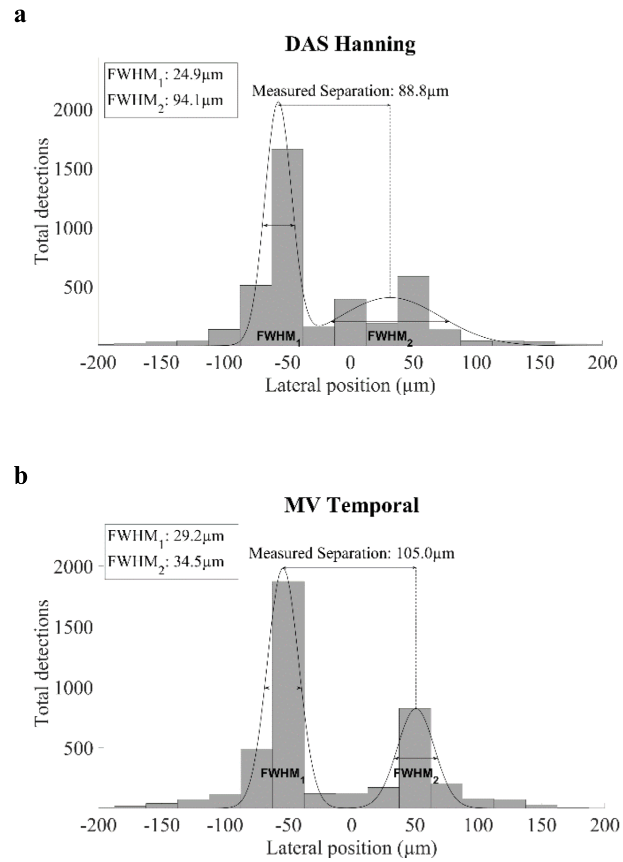

Fig. 3. Resolution of vessel-pair at a separation of 100μm (0.52λ): a) DAS Hanning, (b) MVT.

This theoretical investigation shows for the first time that an adaptive BF, such as the MV, has an advantage for improved vessel definition and vessel resolution compared to a DAS beamformer specifically in the approximate distance range between sub-λ to 4λ. The improved performance of the MV over the DAS is due to the better localisations and increased number of detections leading to the ability to resolve two particles at less than one λ [6]. Also, the larger PSF sizes provided by DAS BFs increase the likelihood of spurious detections, reduced TDs and compromised LU, which lead to a compromised definition and delineation of microvessels.

These advantages of the MV BF are important for a consistent performance of ULM across the image. Note that, a target for super-resolution ultrasound is the early detection of solid tumours that often differ from normal tissue due to the onset of angiogenesis [13], with sub-mm vessel diameters and separation [11]. The results here show that it is in these areas that the DAS BFs are likely to underperform, thus misrepresenting the microvascular density and flow, while the MV BF may help differentiate these microvessels thus improving differentiating tumorous vascular patterns. As a final note, it is important to mention that although the

MV requires several orders of magnitude more calculations compared to the DAS, it has been shown to be feasible with current computing power for live imaging.

4. CONCLUSION

This work theoretically compares the performance of different known BFs when used in combination with ULM. The focus was on vessel recovery for a simplified model of microcirculatory flow as well as a simplified MB behaviour. The MV BF was shown to provide improved microvessel localisation and vessel separation estimation compared to conventional DAS BFs particularly in the range of sub-λ to 4λ. The smaller PSF of the MV BF enabled superior MB detection and localisation compared to DAS BFs and it is these attributes that aided the improved vessel localisation.

5. REFERENCES

1. V. Sboros, C. M. Moran, S. D. Pye, and W. N. McDicken, "The behaviour of individual contrast agent microbubbles," (in eng), Ultrasound Med Biol, vol. 29, no. 5, pp. 687-94, May 2003.
2. K. Thomenius, Evolution of ultrasound beamformers. 1996, pp. 1615-1622 vol.2.
3. V. Perrot, M. Polichetti, F. Varray, and D. Garcia, "So you think you can DAS? A viewpoint on delay-and-sum beamforming," Ultrasonics, vol. 111, p. 106309, 2021/03/01/ 2021, doi: https://doi.org/10.1016/j.ultras.2020.106309.
4. J. F. Synnevag, A. Austeng, and S. Holm, "Adaptive Beamforming Applied to Medical Ultrasound Imaging," IEEE Transactions on Ultrasonics, Ferroelectrics, and Frequency Control, vol. 54, no. 8, pp. 1606-1613, 2007, doi: 10.1109/TUFFC.2007.431.
5. Z. Wang, J. Li, and R. Wu, "Time-delay- and time-reversal-based robust Capon beamformers for ultrasound imaging," (in eng), IEEE Trans Med Imaging, vol. 24, no. 10, pp. 1308-22, Oct 2005, doi: 10.1109/tmi.2005.857222.
6. K. Diamantis, T. Anderson, M. B. Butler, C. A. Villagomez-Hoyos, J. A. Jensen, and V. Sboros, "Resolving Ultrasound Contrast Microbubbles Using Minimum Variance Beamforming," (in eng), IEEE Trans Med Imaging, vol. 38, no. 1, pp. 194-204, Jan 2019, doi: 10.1109/tmi.2018.2859262.
7. K. Diamantis, A. Greenaway, T. Anderson, J. A. Jensen, and V. Sboros, "Experimental performance assessment of the sub-band minimum variance beamformer for ultrasound imaging," Ultrasonics, vol. 79, pp. 87-95, 2017/08/01/ 2017, doi: https://doi.org/10.1016/j.ultras.2017.04.011.
8. A. Boujelben et al., "Multimodality imaging and mathematical modelling of drug delivery to glioblastomas," Interface Focus, Article vol. 6, no. 5, 10/6 2016, doi: 10.1098/rsfs.2016.0039.
9. J. A. Jensen, "Field: A Program for Simulating Ultrasound Systems," (in eng), Medical and Biological Engineering and Computing, vol. 34, no. sup. 1, pp. 351-353, 1997.
10. J. A. Jensen and N. B. Svendsen, "Calculation of pressure fields from arbitrarily shaped, apodized, and excited ultrasound transducers," IEEE Transactions on Ultrasonics, Ferroelectrics, and Frequency Control, vol. 39, no. 2, pp. 262-267, 1992, doi: 10.1109/58.139123.
11. E. Kanoulas et al., "Super-Resolution Contrast-Enhanced Ultrasound Methodology for the Identification of In Vivo Vascular Dynamics in 2D," (in eng), Investigative radiology, vol. 54, no. 8, pp. 500-516, 2019, doi: 10.1097/RLI.0000000000000565.
12. X. Yang, H. Li, and X. Zhou, "Nuclei Segmentation Using Marker-Controlled Watershed, Tracking Using Mean-Shift, and Kalman Filter in Time-Lapse Microscopy," IEEE Transactions on Circuits and Systems I: Regular Papers, vol. 53, no. 11, pp. 2405-2414, 2006, doi: 10.1109/TCSI.2006.884469.
13. G. Russo, M. Mischi, W. Scheepens, J. J. De la Rosette, and H. Wijkstra, "Angiogenesis in prostate cancer: onset, progression and imaging," (in eng), BJU Int, vol. 110, no. 11 Pt C, pp. E794-808, Dec 2012, doi: 10.1111/j.1464-410X.2012.11444.x.